Supplementary information for

Detecting and predicting vegetation transitions based on resilience dynamics and land cover changes

Xueming Zhao [1, 2], Zhaoju Zheng [1], Shijie Yang[1, 2], Dan Zhao[1, 2], Cong Xu[1], Yuan Zeng[1, 2*]

[1] State Key Laboratory of Remote Sensing and Digital Earth, Aerospace Information Research Institute, Chinese Academy of Sciences, Beijing 100101, China
[2] College of Resources and Environment, University of Chinese Academy of Sciences, Beijing 100049, China
* Correspondence: Yuan Zeng; zengyuan@aircas.ac.cn

Table S1. Descriptions of all the potential explanatory variables of five groups. The depth of 0–30cm included three layers of original soil properties data: 0–5cm, 5–15 cm and 15–30 cm. Variables with blue background representing the dynamic variables.

Category	Abbreviation	Spatial resolution	Variable Description	Formula/Model	Data resource/ Organization
Climate	MMP (mm)	1 km	Monthly Mean Precipitation	N/A	Northwest A&F University https://doi.org/10.5281/zenodo.3114194
	MMT (°C)		Monthly Mean Temperature	N/A	Northwest A&F University https://doi.org/10.5281/zenodo.3185722
	PET (mm)		Monthly Potential evapotranspiration	N/A	Northwest A&F University https://doi.org/10.11866/db.loess.2021.001
	AI		Aridity index	PET/MMP	N/A
	SPEI		The Standardized Precipitation Evapotranspiration Index	N/A	Beijing Normal University https://zenodo.org/record/8312201
Vegetation characteristics	FVC (%)	250 m	Fractional Vegetation Cover	Pixel binary model $FVC = \frac{NDVI - NDVI_{soil}}{NDVI_{veg} - NDVI_{soil}}$	Google Earth Engine platform

	SAVI		Soil Adjusted Vegetation Index	calculated from MOD09Q1 $SAVI = \frac{1.5 * (Nir - Red)}{Nir + Red + 0.5}$ calculated from MOD09Q1	
	EVI		Enhanced Vegetation Index	EVI band of MOD13Q1	
	LAI		Leaf Area Index	LAI band of MCD15A2	
	NPP (gC/m²)		Net Primary Production	LSWI-based CASA model [1]	Inner Mongolia Normal University
	AGB (g/m²)		Aboveground Biomass	Machine learning models [2]	Chinese Academy of Agricultural Sciences
	Richness	5 km	Richness	N/A	University of Bologna https://doi.org/10.25829/idiv.3506-p4c0mo
	FCH (m)	250 m	Forest Canopy Height	Neural network guided interpolation method [3]	Peking University www.3decology.org/dataset-software
	FA (year)	30 m	Forest Age	Machine learning models [4]	Fujian Normal University https://doi.org/10.6084/m9.figshare.24464170
Soil Properties	pH	250 m	soil pH (H2O), 0–30 cm	$-\log_{10}((5 * 10^{-pH_{0-5}} + 10 * 10^{-pH_{5-15}}$	Institute of Soil Science, Chinese Academy of Sciences

				$+15 * 10^{-pH_{15-30}})/30))$	http://soil.geodata.cn/data/datadetails.html?dataguid=36810085119113
	SOC (g/Kg)		Soil Organic Carbon, 0–30 cm	$(5 * Soil_{0-5} + 10 * Soil_{5-15} + 15 * Soil_{15-30})/30$	
	TN (g/Kg)		Total Nitrogen, 0–30 cm		
	TP (g/Kg)		Total Phosphorus, 0–30 cm		
	TK (g/Kg)		Total Potassium, 0–30 cm		
	Thickness (cm)		Thickness, 0–20 cm		
Topography	DEM (m)	30 m	Digital Elevation Model	N/A	NASA and METI https://doi.org/10.5067/ASTER/ASTGTM.003
	Slope (°)		Slope	calculated based on DEM	
Human activities	POP (people/km²)	1 km	Population Density	Raster spatial calculation [5]	Institute of Geographic Sciences and Natural Resources Research, Chinese Academy of Sciences https://doi.org/10.12078/2017121101
	Graze (SU/ha)	0.0025°	Grazing Intensity	Machine learning models [6]	Peking University https://doi.org/10.6084/m9.figshare.26195684

$NDVI_{soil}$ and $NDVI_{veg}$ represent the NDVI value of a purely bare soil pixel and a pixel fully covered by vegetation based on the 5th and 95th percentiles of the

NDVI distribution within the study area, respectively. Nir and Red represent the near-infrared and red spectral band of MOD09Q1 data.

Table S2. The detailed information of temporal cross-validation of a 4-year lead time using 10 years of training data.

Model Type	Train year	Train window	Train samples	Test year	Test window	Test samples
Forest	2013	2000 ~ 2009	606	2014	2001 ~ 2010	588
	2014	2001 ~ 2010	588	2015	2002 ~ 2011	442
	2015	2002 ~ 2011	442	2016	2003 ~ 2012	772
	2016	2003 ~ 2012	772	2017	2004 ~ 2013	966
	2017	2004 ~ 2013	966	2018	2005 ~ 2014	1052
Grassland	2013	2000 ~ 2009	748	2014	2001 ~ 2010	1124
	2014	2001 ~ 2010	1124	2015	2002 ~ 2011	1224
	2015	2002 ~ 2011	1224	2016	2003 ~ 2012	1664
	2016	2003 ~ 2012	1664	2017	2004 ~ 2013	1370
	2017	2004 ~ 2013	1370	2018	2005 ~ 2014	1428

Table S3. Spatial density of detected tipping points pixels for each ecoregion.

Ecoregions	Spatial density of detected tipping points (per 10000 km^2)
Cold temperate needleleaf forest	1.5
Temperate needleleaf broadleaf mixed forest	0.91
Warm temperate deciduous broadleaf forest	18.80
Subtropical evergreen broadleaf forest	12.19
Tropical rain forest	4.71
Temperate steppe	8.78
Temperate desert	3.25
The Qinghai-Tibetan Plateau alpine vegetation	6.83

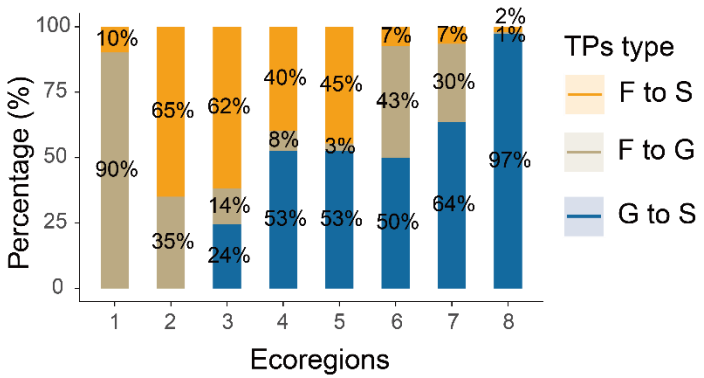


Figure S1. Percentage of different types of tipping points (TPs) within each ecoregion. The percentage represents the relative proportion of different types of vegetation transitions (F to S: forest to shrubland, F to G: forest to grassland, and G to S: grassland to shrubland) out of the total tipping points detected within each region. Numbers on the x-axis indicate: 1. CTempNLF: cold temperate needleleaf forest; 2. TempNBMF: temperate needleleaf broadleaf mixed forest; 3. WTempDBF: warm temperate deciduous broadleaf forest; 4. SubtroEBF: subtropical evergreen broadleaf forest; 5. TroRF: tropical rain forest; 6. TempS: temperate steppe; 7. TempD: temperate desert; 8. QTPVege: the Qinghai-Tibetan Plateau alpine vegetation.

References

1. Bao, G.; Y. Bao; Z. Qin; X. Xin; Y. Bao; S. Bayarsaikan; Y. Zhou; B. Chuntai. Modeling net primary productivity of terrestrial ecosystems in the semi-arid climate of the Mongolian Plateau using LSWI-based CASA ecosystem model. Int. J. Appl. Earth Obs. Geoinf. 2016, 46, 84-93, doi:10.1016/j.jag.2015.12.001.
2. Li, H.; F. Li; J. Xiao; J. Chen; K. Lin; G. Bao; A. Liu; G. Wei. A machine learning scheme for estimating fine-resolution grassland aboveground biomass over China with Sentinel-1/2 satellite images. Remote Sens. Environ. 2024, 311, doi:10.1016/j.rse.2024.114317.
3. Liu, X.; et al. Neural network guided interpolation for mapping canopy height of China's forests by integrating GEDI and ICESat-2 data. Remote Sens. Environ. 2022, 269, doi:10.1016/j.rse.2021.112844.
4. Lin, X.; Shang, R.; Chen, J.M.; Zhao, G.; Zhang, X.; Huang, Y.; Yu, G.; He, N.; Xu, L.; Jiao, W. High-resolution forest age mapping based on forest height maps derived from GEDI and ICESat-2 space-borne lidar data. Agric. For. Meteorol. 2023, 339, 109592. https://doi.org/10.1016/j.agrformet.2023.109592.
5. Xu, X. China Population Spatial Distribution Kilometer Grid DataSet. 2017, doi:10.12078/2017121101.
6. Wang, D.; Q. Peng; X. Li; W. Zhang; X. Xia; Z. Qin; P. Ren; S. Liang; W. Yuan. A long-term high-resolution dataset of grasslands grazing intensity in China. Sci. Data 2024, 11(1), doi:10.1038/s41597-024-04045-x.